Hydrology and
Earth System
Sciences
Discussions

Open Access

Shift of annual water balance in the Budyko space for a catchment with groundwater dependent evapotranspiration

X.-S. Wang[1] and Y. Zhou[2]

[1]Ministry of Education Key Laboratory of Groundwater Circulation and Evolution, China University of Geosciences, Beijing 100083, China
[2]UNESCO–IHE Institute for Water Education, Delft, the Netherlands

Correspondence to: X.-S. Wang (wxsh@cugb.edu.cn)

HESSD

12, 11613–11650, 2015

Shift of annual water balance in the Budyko space

X.-S. Wang and Y. Zhou

Title Page

Abstract | Introduction

Conclusions | References

Tables | Figures

◀◀ | ▶▶

◀ | ▶

Back | Close

Full Screen / Esc

Printer-friendly Version

Interactive Discussion

Abstract

Empirical equations have been formulated for the general relationship between the evapotranspiration ratio (F) and the aridity index (ϕ) in the Budyko framework. Though it is normally applied for mean annual behaviors, the Budyko hypothesis has been directly adopted to analyze the interannual change in water balance. However, there are reported cases where the annual evapotranspiration ratio is larger than 1.0 ($F > 1$). This study reveals the effects of groundwater dependent evapotranspiration in triggering such abnormal shift of annual water balance in the Budyko space. A widely used monthly hydrological model, the ABCD model, is modified to incorporate the groundwater dependent evapotranspiration in the zone with shallow water table and delayed groundwater recharge in the zone with deep water table. This model is applied in the Hailiutu River catchment in China. Results show that the variations in the annual evapotranspiration ratio with aridity index do not satisfy the traditional Budyko hypothesis. The shift of the annual water balance in the Budyko space depends on the proportion of shallow water table area, intensity of groundwater dependent evapotranspiration, and the normal Budyko-type trend of F in the deep groundwater zone. Excess evapotranspiration ($F > 1$) could occur in extreme dry years, which is enhanced by groundwater-dependent evapotranspiration. Use of groundwater for irrigation may increase the frequency of occurrence of the $F > 1$ cases.

1 Introduction

Estimating catchment water balance is one of the fundamental tasks in hydrology. Efforts have long been devoted to construct physical, empirical, and statistical models to explain the general relationship among precipitation (P), runoff (Q), potential evapotranspiration (E_0) and actual evapotranspiration (E) in terms of mean annual fluxes at the catchment scale (Budyko, 1948, 1958, 1974; Mezentsev, 1955; Fu, 1981; Porporato et al., 2004; Gerrits et al., 2009). A simple and highly intuitive approach widely used for

estimating E at mean annual scale is the Budyko framework, in which the mean annual evapotranspiration ratio (E/P) was presumed as a function of the climatic dryness as:

$$\frac{E}{P} = F\left(\frac{E_0}{P}\right) = F(\phi),\tag{1}$$

where ϕ is the aridity index defined as E_0/P, and $F(\phi)$ is an empirical function that relates E/P to ϕ based on general water-energy balance behaviors in catchments. The proposed formula by Budyko (1958, 1974) was:

$$F(\phi) = \sqrt{\phi[1 - \exp(-\phi)]\tanh(1/\phi)},\tag{2}$$

which indicates a nonlinear relation between F and ϕ. This $F-\phi$ curve has been called the Budyko curve (Zhang et al., 2004; Roderick and Farquhar, 2011) and the $F-\phi$ space was called Budyko space (Renner et al., 2012).

Instead of using a single curve determined by Eq. (2) in the Budyko space, researchers have introduced a specific catchment parameter in $F(\phi)$ to consider the impacts of catchment properties such as soils and vegetation. Mezentsev (1955) proposed:

$$F(\phi) = \frac{\phi}{(1 + \phi^n)^{1/n}},\tag{3}$$

where n is a dimensionless parameter which was related to the catchment landscape characteristics. Following the idea of Mezentsev (1955), Fu (1981) derived a new semi-empirical formula for the $F-\phi$ relationship that was published in Chinese and later used by Zhang et al. (2004):

$$F(\phi) = 1 + \phi - (1 + \phi^\omega)^{1/\omega},\tag{4}$$

where ω is a catchment parameter, which synthetically represents the negative features for runoff producing (Fu, 1981). Fu's equation has been widely used in the last

X.-S. Wang and Y. Zhou

decade (Zhang et al., 2004, 2008; Yang et al., 2006, 2007; Greve et al., 2015). In addition, Zhang et al. (2001) presented an empirical equation for the Budyko framework in relation to vegetation cover at the catchment scale as:

$$F(\phi) = \frac{w\phi}{1 + w\phi + \phi^{-1}}, \tag{5}$$

where w is called the plant-available water coefficient. Recently, Wang and Tang (2014) also developed a one-parameter Budyko model based on the proportionality hypothesis.

Budyko hypothesis has been directly used to analyze the interannual change in water balance in catchments (Arora, 2002; Zhang et al., 2008; Potter and Zhang, 2009) even through it is normally applied for mean annual behaviors. One can plot annually the estimated E/P data in the Budyko space to check whether the normal Budyko curves are sufficient or not to represent the interannual variability of evapotranspiration with varying dryness. By this way, Potter and Zhang (2009) found that the Budyko model is generally applicable for the catchments in Australia and the optimal curve of annual E/P vs. ϕ is highly dependent on seasonal variation in rainfall. However, this approach should be carefully used when the E/P values are approximated by $(P - Q)/P$ values. Wang et al. (2009) and Istanbulluoglu et al. (2012) reported that the annual data of $(P - Q)/P$ in some basins are negatively related to the aridity index, exhibiting an inverse trend in comparison with the normal Budyko curves. According to long-term groundwater observation in the North Loup River basin (NLRB), Nebraska, USA, Istanbulluoglu et al. (2012) demonstrated that the annual E/P values estimated by $(P - Q - \Delta G)/P$ basically follows the Budyko hypothesis where ΔG is the change in groundwater storage.

Recently, unexpected high evapotranspiration ratio ($E/P > 1$) was observed (L. Cheng et al., 2011; Wang, 2012; X. Chen et al., 2013) which could not be interpreted by the conventional Budyko curves. Among the 12 watersheds investigated in Wang (2012), half of them exhibited such high E/P values in two or more dry years.

The physical base of the phenomena is the significant contribution of storage in extremely arid situation by which the high level of evapotranspiration is maintained. Although some of the cases was due to extracting groundwater for irrigation in farmlands (Cheng et al., 2011; Wang, 2012), it could happen in natural conditions as a result of the temporal redistribution of water from seasonal patterns (Chen et al., 2013). The excess annual evapotranspiration over the annual precipitation may be originated from both soil water and groundwater. As reported by Wang (2012), during the drought year in 1988, two watersheds in Illinois, USA, showed $E/P = 1.1$ with $\sim 100\,\text{mm}$ depletion in soil water and $\sim 200\,\text{mm}$ decrease in groundwater storage, respectively. It seemed that the contribution of groundwater is more significant (partially enhanced by pumping). Small depth to water table is an advantage to keep a high level of soil water content near ground surface for evapotranspiration (Chen and Hu, 2004). Therefore, it could be argued that the existence of shallow groundwater in a catchment would enhance the occurrence of $E/P > 1$ in dry years. Groundwater dependent evapotranspiration at the regional scale has been noticed in a few of the previous studies (York et al., 2002; Chen and Hu, 2004; Cohen et al., 2006; Yeh and Famiglietti, 2009). Nevertheless, little has been known on the role of groundwater in the interannual variability of the evapotranspiration ratio with varying dryness.

This study aims to advance the understanding of the interannual variability of water balance in the Budyko space for catchments with groundwater dependent runoff and evapotranspiration. At the first, a monthly hydrological model was developed from the widely used ABCD model (Thomas, 1981) to incorporate the groundwater dependent evapotranspiration as well as the deep infiltration in the vadose zone. Then, the modified model was applied to the Hailiutu River Catchment (HRC) in the Erdos Plateau of central China as an example. The calibrated model was used to produce the annual data of evapotranspiration components which are linked with variable soil water and groundwater storage. With varying climatic dryness, the shift behaviors of the interannual water balance in the Budyko space for the catchment were analyzed in detail. The impacts of human activities were also discussed. The study reveals the contribution of

groundwater in the interannual variability of catchment water balance under a changing climate.

2 Hydroclimatologic models

2.1 The ABCD model

The ABCD model is a conceptual hydrological model with 4 parameters (a, b, c, and d) developed by Thomas (1981) to account for the actual evapotranspiration, surface and sub-surface runoff, and storage changes. The ABCD model was originally applied at an annual time step but has been recommended as a monthly hydrological model (Alley, 1984). It was widely applied as a hydroclimatologic model to investigate the response of catchments on climate change (Vandewiele et al., 1992; Fernandez et al., 2000; Sankarasubramanian and Vogel, 2002; Li and Sankarasubramanian, 2012).

Both soil water and groundwater storages are considered in the model, as shown in Fig. 1a. At the monthly time step, the change in soil water storage is determined by

$$S_m - S_{m-1} = P_m - E_m - R_m, \tag{6}$$

where S_{m-1} and S_m are the effective soil water storage at the beginning and the end of the mth month, respectively; P_m and E_m are the monthly precipitation and evapotranspiration values, respectively; and R_m is the monthly loss of soil water via direct runoff and groundwater recharge. The change in groundwater storage is determined by

$$G_m - G_{m-1} = cR_m - dG_m, \tag{7}$$

where G_{m-1} and G_m represent the groundwater storage at the beginning and the end of the mth month, respectively; and c and d are two parameters that account for groundwater recharge and discharge from R_m and G_m, respectively. The monthly streamflow is the summation of the monthly direct runoff and groundwater discharge, as follows:

$$Q_m = (1 - c)R_m + dG_m. \tag{8}$$

The change in storage in the ABCD model is the summation of the changes in soil water storage and groundwater storage, which can be expressed as $W_m - W_{m-1} = (S_m - S_{m-1}) + (G_m - G_{m-1})$.

Thomas (1981) proposed a nonlinear function to estimate $(E_m + S_m)$ from $(P_m + S_{m-1})$ as follows:

$$E_m + S_m = \frac{P_m + S_{m-1} + b}{2a} - \sqrt{\left(\frac{P_m + S_{m-1} + b}{2a}\right)^2 - \frac{(P_m + S_{m-1})b}{a}}, \qquad (9)$$

where a is a dimensionless parameter, and b is the upper limit of $(E_m + S_m)$. In addition, *Thomas* (1981) assumed

$$S_m = (E_m + S_m)\exp(-E_{0\,m}/b), \qquad (10)$$

where $E_{0\,m}$ is the monthly potential evaporation for the mth month. Substituting Eq. (10) into Eq. (9), the monthly evapotranspiration can be estimated as

$$E_m = \left[\frac{P_m + S_{m-1} + b}{2a} - \sqrt{\left(\frac{P_m + S_{m-1} + b}{2a}\right)^2 - \frac{(P_m + S_{m-1})b}{a}}\right]\left[1 - \exp\left(-\frac{E_{0\,m}}{b}\right)\right]. \tag{11}$$

Wang and Tang (2014) demonstrated that Eq. (9) can be derived from the generalized proportionality principle and yield an equivalent Budyko-type model.

2.2 The ABCD-GE model

To investigate the effects of groundwater dependent runoff and evapotranspiration in basins with both shallow and deep groundwater, the original ABCD model is extended in this study as the ABCD-GE model where GE denotes groundwater dependent evapotranspiration. As shown in Fig. 1b, a catchment is conceptually divided into two zones

where the Zone-1 and Zone-2 represent different areas with deep and shallow groundwater, respectively. Surface water is also included in the Zone-2. The soil water reservoir in the Zone-1 is the same as that in the ABCD model whereas no direct runoff occurs on its surface. In addition, a transition vadose zone is specified between the soil layer and water table to represent the delayed groundwater recharge. In the Zone-2, rainfall and evapotranspiration are the components directly involved in the water balance of groundwater as well as the surface runoff. Thus, three storage components are considered as a chain in the hydrological processes.

In the ABCD-GE model, direct runoff only occurs in the Zone-2 and is assumed to be proportional to the precipitation as $(1-c)P_m$ where c is similar to the dimensionless parameter used in the ABCD model but now is linked with the precipitation. The total runoff in the catchment is the sum of the direct runoff and groundwater discharge as follows

$$Q_m = \alpha(1-c)P_m + dG_m, \tag{12}$$

where α is the ratio of the area Zone-2 to the area of the whole catchment. In comparison with Eq. (8), herein the direct runoff is estimated with the amount of precipitation (αP_m) in the Zone-2, rather than with R_m.

Similar to that in the ABCD model, the change in the soil water storage is determined by

$$S_m - S_{m-1} = P_m - E_{1\,m} - R_m, \tag{13}$$

where $E_{1\,m}$ is the monthly evapotranspiration in the Zone-1 dependent on Eq. (11), R_m becomes the monthly leakage of soil water, forming the recharge to the transition vadose zone in the Zone-1. The change in this vadose zone storage is described with

$$V_m - V_{m-1} = R_m - kV_m, \tag{14}$$

where V_m and V_{m-1} represent the storages in the transition vadose zone at the end and beginning of the mth month, respectively, and k is the parameter that accounts

for groundwater recharge rate as kV_m. In considering of the gain-loss processes of groundwater, the change in the effective groundwater storage is yielded by

$$G_m - G_{m-1} = (1 - \alpha)kV_m + \alpha(cP_m - E_{2\,m}) - dG_m, \tag{15}$$

where $E_{2\,m}$ is the monthly evapotranspiration in the Zone-2, which depends on the effective groundwater storage as follow

$$E_{2\,m} = gG_mE_{0\,m}, \tag{16}$$

where g is a parameter controlling the intensity of groundwater dependent evapotranspiration. Equation (16) assumes that the evapotranspiration rate in the Zone-2 is simply proportional to both the groundwater storage (which is positively related to groundwater level) and the potential evapotranspiration rate. Thus, the evapotranspiration rate as a whole in the catchment is summarized as

$$E_m = (1 - \alpha)E_{1\,m} + \alpha E_{2\,m}. \tag{17}$$

Equations (13)–(15) are solved one by one and finally the value of G_m is substituting into Eq. (12) to obtain the runoff. The solutions of the ABCD-GE model are controlled by 7 parameters as: a, b, c, d, g, k and α.

3   Study site, data and model calibration

3.1   Study area

The study site is the Hailiutu River catchment (HRC), with an area of 2645 km², located in the Erdos Plateau in north-central China (Fig. 2a). The HRC lies on the southeast edge of the Mu Us Desert and is a sub-catchment of the Wuding River basin, which drains into the Yellow River (Fig. 2b). The climate of the Erdos Plateau is typically inland semiarid to arid. The mean annual precipitation in the HRC is $\sim 350\,\mathrm{mm\,a^{-1}}$.

Full Screen / Esc

Printer-friendly Version

Interactive Discussion

X.-S. Wang and Y. Zhou

More than 60 % of the annual precipitation is received in the warm season (June, July, August and September). The land cover within the catchment is characterized by desert sand dunes with patches of mostly shrub-grassland. The main channel of the HRC has a length of approximately 85 km and flows southwards to the Hanjiamao hydrological station, as shown in Fig. 2c. Due to the arid climate and desert landscape, vegetation cover in the HRC is sparse. *Salix psammophila* (shrubs) and *Artemisia desertorum* (grasses) are the dominant plants on the sand dunes. Depression areas and terrace lands with shallow groundwater are covered by grasses. Wind-breaking trees (*Salix matsudana* and *Populus tomentosa*) can be found along the roads and crop areas. Farmlands are mainly located in the southern area and especially in the river valley. Crops cover only ∼ 3 % of the total catchment area. Maize is the dominant crop and is irrigated with streamflow and/or groundwater. Several diversion dams have been constructed along the Hailiutu River since the early 1970s for irrigation.

Regional groundwater level distribution in the study area has been investigated in Lv et al. (2013) based on a hydrogeological survey carried out in 2010. According to this investigation, depth to water table (DWT) in the area varies in a large range up to 110 m. Figure 3 shows the histogram of DWT based on the 300 m-resolution gridded data of groundwater level (Lv et al., 2013). In more than half of the area, DWT is less than 10 m. The shallow groundwater zone, where DWT is no more than 2 m, occupies the 16.0 % of the whole catchment area. As investigated in Yin et al. (2015) at the site of the HRC, when DWT is less than 2 m, the transpiration rate of trees is generally higher than 90 % of the potential transpiration rate and the soil surface evaporation rate is generally higher than 60 % of the potential. As a whole, the evapotranspiration rate would be generally higher than 80 % of the potential when DWT is less than 2 m, whereas the evapotranspiration ratio is generally less than 0.4 for the deep groundwater condition (Yin et al., 2015). This investigation confirms that groundwater dependent evapotranspiration is an essential process in the HRC.

3.2 Data

Daily streamflow data since 1957 is available from the Hanjiamao hydrological station. A rainfall gauge was also installed at the hydrological station in 1961, providing daily data of precipitation. In addition to the Hanjiamao station, rainfall is observed at the city of Uxin Qi, located in the northern half of the basin (Fig. 2c), where a meteorological station has been in operation since 1961.

Because of the limitations of only two rainfall gauges in a relatively large area and to better account for the variability of monthly rainfall in space and time, we used gridded monthly precipitation data. We developed gridded precipitation data with 1 km resolution between 1957 and 2010 by using rainfall data from 14 national meteorological stations on the Erdos Plateau (Fig. 2b). Monthly rainfall data at these 14 stations were downloaded from the China Meteorological Data Sharing Service System (CMDSSS, http://cdc.nmic.cn). We constructed the gridded monthly data using the inverse distance square weighting (IDSW) method due to the moderate topography of the Erdos Plateau in the form of low-relief rolling hills. Figure 2b shows the mean annual precipitation contours of the Erdos Plateau obtained from the gridded data. Within the HRC, precipitation is relatively uniformly distributed (Yang et al., 2012) because of the flat topography of the region, but a subtle ($\sim$ 40 mm) increase in precipitation from north to south across the basin can be observed in Fig. 2b. In this study, the area-averaged monthly precipitation in the HRC for the period 1963–2010 was estimated by imposing the basin boundaries on the gridded monthly precipitation data and taking the arithmetic average of the grid cells within the HRC boundaries.

The method applied in constructing the gridded precipitation data were further applied in constructing a 1 km resolution gridded data set for monthly pan evaporation between 1957 and 2010 for the Erdos Plateau. The pan evaporation data were based on observations from 200 mm diameter pans that were installed in most stations on the Erdos Plateau and can also be downloaded from CMDSSS (http://cdc.nmic.cn). The average monthly potential evapotranspiration (E_0) in the HRC was estimated from the

spatially averaged data of pan evaporation using a local pan coefficient (0.58) for the 200 mm diameter pan. This coefficient was suggested by various investigations of pan coefficients for Chinese meteorological stations (Shi et al., 1986; Fan et al., 2006).

In Fig. 4a, the variation patterns of the monthly rainfall and potential evapotranspiration at the catchment scale during 1957–2010 are shown. Both rainfall and evapotranspiration are high in the summer and low in the winter. However, there is a difference in the patterns which may influence the seasonal variation in runoff: the rainfall peak normally arrives in the August but the highest evaporation is exhibited in the June. With respect to these meteorological patterns, the total runoff drops in the Spring and in the early Summer until the heavy rainfall coming in the August, as shown in Fig. 4b. In comparison with the rainfall and the potential evapotranspiration, the mean monthly runoff (2.6 mm) and its fluctuation magnitude (0.8–11.9 mm) are quite small. This indicates that most of the precipitation in the HRC returns to the atmosphere by evapotranspiration. During 1957 to 2010, the mean annual P and Q are 350 and 32 mm, respectively. The runoff ratio is $Q/P \approx 0.09$. The mean annual potential evaporation in this period is $E_0 = 1248\,\mathrm{mm\,a^{-1}}$, indicating a mean aridity index of $\phi \approx 3.6$. The annual aridity index in this period generally ranged between 2 and 7, covering the semiarid and arid climatic conditions as classified in the scheme recommended by the United Nations Environment Programme (UNEP) (Middleton and Thomas, 1992).

In the HRC, there are interannual fluctuations in E_0, P, and Q. However, no significant trends were detected in E_0 and P, whereas several regime shifts were detected in Q. Yang et al. (2012) found that the annual regime shifts in streamflow were caused largely by land use policy changes and river water diversions for irrigation. Table 1 shows the mean annual fluxes in four typical periods with different numbers of diversions in the Hailiutu River and major branches during 1957–2010. These diversions influenced the hydrological behavior in the HRC and will be discussed in the following sections. However, before 1967, the Hailiutu River was free of hydraulic engineering, and the studied area was close to natural conditions.

3.3 Model calibration

We applied the ABCD-GE model to estimate the monthly evapotranspiration and the change in storage in the HRC with the calibrated parameters. The monthly evapotranspiration data were then used to estimate the annual evapotranspiration for further analysis. The model calibration was based on the observed monthly streamflow data at the Hanjiamao station and the separated base flow data.

Because groundwater discharge has been included in the model, a base flow analysis was performed to obtain the expected groundwater discharge for the model calibration. Using the automated hydrograph separation method HYSEP (Sloto and Crouse, 1996) on the daily streamflow data, such "observed" groundwater discharge data were obtained for the period 1957–2010. These data were partly reported in Zhou et al. (2013). The base flow index ranges between 0.80 and 0.95 for annual streamflow, indicating that groundwater flow is the dominant hydrological process in the HRC. Variation patterns of the monthly groundwater discharge are shown in Fig. 4b.

The ordinary least squares (OLS) criterion was applied for parameter estimation. The errors of both log-streamflow and log-base-flow were included in the OLS objective function, as follows:

$$\min U = \sum_{m=1}^{N} \left(e_m^2 + q_m^2 \right), \tag{18}$$

where

$$e_m = \ln(\hat{Q}/Q)_m, \quad q_m = \ln(\hat{Q}_b/Q_b)_m, \tag{19}$$

and U is the value of the objective function; N is the number of months; $\hat{Q}$ and Q are the simulated and observed monthly streamflow, respectively; $\hat{Q}_b$ is the simulated monthly groundwater discharge through dG_m in Eq. (12); and Q_b is the "observed" monthly groundwater discharge obtained from the base flow analysis. The log form errors given

in Eq. (19) can be used to obtain homoscedastic residuals (rather than the residual errors) of the normal absolute differences between the observed data and the model outputs (Alley, 1984). The nonlinear optimization algorithm Generalized Reduced Gradient (GRG) (Lasdon et al., 1978) was used to determine the optimum values of the parameters. The Nash–Sutcliffe efficiency (NSE) (Nash and Sutcliffe, 1970) was also applied to evaluate the performance of the model. The NSE value ranges in $(-\infty, 1)$ whereas a higher than zero value is required for a well-perform model.

The parameters in the model were firstly identified using the 1957–1966 data, and this calibrated model was considered to be a "natural" model due to the minimum impact of human activities during this 10 years period. The initial storage values were also regarded as the unknown parameters to be determined in the calibration process. Changes in the initial conditions generally influenced the simulated results in the first and second years. Therefore, the residual errors in the later years were applied to estimate the parameter values with less influence from the initial conditions. A sensitivity analysis was carried out to schematically capture the ranges of the parameter values. The best fitting parameter values obtained through the model calibration are shown in Table 2. The a value approximates to 1.0. In previous studies using the ABCD model, the a value was found generally to be higher than 0.9 (Alley, 1984; Sankarasubramanian and Vogel, 2002; Li and Sankarasubramanian, 2012). The b and d values fall into the ranges suggested by Alley (1984). The c value is 0.92, indicating that there are 8 % of the precipitation in the Zone-2 were transferred to direct runoff during the 1957–1966 period. The fractional area of the shallow groundwater zone, α, is 0.21, which was larger than the current area (16.0 %) of the zone with the DWT less than 2 m. Such a difference is reasonable because the groundwater level before 1967 should be higher than that at present as indicated by the decrease trend of the baseflow began from 1967. The k value controls the rate of groundwater recharge below the transition vadose zone. The transition vadose zone is a necessary component in the HRC as demonstrated by the sensitivity analysis on the k value. When an extremely high value of k is used ($k > 100$), the kV_m value would be almost equal to R_m so that the transition

vadose zone does not make sense. However, in this situation the model could never capture the seasonal variation patterns of the runoff and groundwater discharge in the HRC. The best fitting k value is significantly less than 1.0, indicating a strong delay effect. Thus, the delayed groundwater recharge is an essential process in this study area.

For the 1957–1966 period, the mean standard error of the calibrated model is smaller than 15 %. The NSE value of the model is 0.51, not very high but significantly larger than zero. It is usually difficult to obtain a high NSE value for a catchment with weak seasonal variation in runoff (Mathevet et al., 2006). The annual simulation results match the observation much better than the monthly simulation results as indicated by the correlation coefficient (compare Fig. 5a with b). We used this "natural" model to estimate the monthly runoff (Fig. 6a) and groundwater discharge (Fig. 6b) for the whole 1957–2010 periods. The model output monthly runoff after 1966 are higher than the observed values due to ignoring the impacts of land use changes and increased utilization of water for irrigation. However, the simulated patterns of groundwater discharge are similar to the observations: falling in the summer, rising in the autumn. This agreement between the simulated and observed patterns demonstrates the ability of the ABCD-GE model in simulating the hydrological behaviors in the studied catchment: significant groundwater-dependent evapotranspiration occurs in the summer, and a strong recovery of storage in the shallow-groundwater zone occurs in the autumn due to persistent recharge from the thick vadose zone.

For the periods after 1966, the differences between the model calculated natural annual runoff and the observed values as shown in Fig. 6c could be interpreted as the excess evapotranspiration induced by increasing agricultural water use from river diversion. Enhanced evapotranspiration also occurred in the shallow groundwater zone due to groundwater pumping for irrigation. To evaluate the actual water balance, the following equation

$$E_{ACT} \approx E_{NAT} + (Q_{NAT} - Q_{OBS}), \tag{20}$$

Full Screen / Esc

Printer-friendly Version

Interactive Discussion

is applied in an approximate way to estimate the actual annual evapotranspiration (E_{ACT}) after 1966 from the "natural" model result (E_{NAT}) plus the difference of annual runoff between the "natural" model (Q_{NAT}) and the observation (Q_{OBS}). Thus, the irrigation water use in the catchment is included in E_{ACT}. Results are shown in Fig. 6d. It seems that the difference between E_{NAT} and E_{ACT} is not significantly large in comparison with the mean annual evapotranspiration. The maximum $Q_{NAT} - Q_{OBS}$ value is less than 10 % of the mean annual evapotranspiration ($\sim 315\,\text{mm}$). Accordingly, the irrigation water use in the HRC did not significantly influence the annual evapotranspiration at the catchment scale. However, it dramatically influenced the streamflow. As shown in Fig. 6a, almost all of the direct runoff was removed from the total runoff after 1987 and groundwater discharge was significantly decreased even though the seasonal patterns were basically remained (Fig. 6b).

4   Results and discussions

4.1   Interannual variability of the HRC in the Budyko space

In Fig. 7a, the E_0/P and E/P data for the annual water balance obtained from the "natural" model over this 55 years period are plotted in the Budyko space. For comparison, the results of the actual evapotranspiration (including irrigation) obtained with Eq. (16) are plotted as well. The E/P values obtained from the "natural" model is a little bit lower than that including irrigation. For both data sets, with increase in the aridity index, the evapotranspiration ratio ($F = E/P$) increases almost linearly with the R-square as high as 0.88. When ϕ is larger than 4, the evapotranspiration ratios fall above the line of $F = 1$. Since $F = 1$ is the bound of the mean annual evapotranspiration ratio predicted by the traditional Budyko hypothesis, the occurrence of such high F values indicates that the traditional Budyko formulas, shown in Eqs. (2)–(5), cannot be applied in analyzing the annual water balance in the HRC. During extreme dry years when $\phi > 4$, the annual precipitation is generally less than 290 mm whereas the annual evapotranspi-

ration is generally higher than 300 mm. The excess evapotranspiration is sustained by shallow groundwater.

For mean annual water balance, as indicated in the traditional Budyko framework, the runoff ratio (Q/P) would decrease with increase in the aridity index. It is represented by a decay curve in the Q/P vs. ϕ plot. However, the annual runoff ratio in the HRC shows an opposite trend (Fig. 7b). The annual runoff ratio obtained from the "natural" model increases almost linearly with increasing aridity index. The reason for this positive trend is also the large contribution of groundwater storage to river discharge during the extreme dry years. The runoff ratio was decreased in actual due to irrigation water use, which weakened the linear relationship but remained the increase trend of Q/P vs. ϕ.

The effects of groundwater dependent evapotranspiration can be clearly observed when the evapotranspiration ratio is divided into two parts and plotted in the Budyko space separately with respect to the shallow and deep groundwater zones, as shown in Fig. 8. It is obvious that the annual E_1/P values in the Zone-1 (deep groundwater) for the whole range of the aridity index are smaller than 1.0 and fall below the Budyko curve determined by Eq. (2). The low E_1/P value in the Zone-1 is mainly due to the deep water table condition. Since the water table is deep, large portion of precipitation converts to effective groundwater recharge. The land covers in the deep groundwater zone are dominated by sparse desert grasses which have much lower evapotranspiration rates. The E_1/P trend can be sufficiently fitted by the Budyko curve determined with Eq. (5) for $w = 0.5$. As suggested by Zhang et al. (2001), the plant-available water coefficient, w, ranges between 0.5 and 2.0 where the lower limit refers to short grass or pasture, satisfying the situation in the HRC. However, the relationship between the annual evapotranspiration ratio and the annual aridity index in the shallow groundwater zone definitely could not be explained by any of the existing Budyko formulas, because all the annual F values for the Zone-2 are higher than 1.0. The E_2/P value increases from 1 to 7 when the ϕ value increases from 1.5 to 9.8, approximately following a linear trend. This trend agrees with the relationship between E_2 and E_0 ($E_2 \propto E_0$)

Shift of annual water balance in the Budyko space

X.-S. Wang and Y. Zhou

Title Page

Abstract | Introduction

Conclusions | References

Tables | Figures

◀ | ▶|

◀ | ▶

Back | Close

Full Screen / Esc

that described in Eq. (16). When the groundwater storage, G, is relatively stable, the annual E_2/P value would be proportional to the annual E_0/P value and the slope is represented by the annual mean value of gG. In the HRC, the annual mean value of gG is 0.65 according to the "natural" model. Thus, the annual E_2/P value must be higher than 1.0 when ϕ is higher than 1.5. Such a groundwater dependent evapotranspiration process is the reason for the cases of $F > 1$ occurred at the catchment scale in the HRC.

4.2 Controls on the $F > 1$ cases

It has been demonstrated in Fig. 7a that the annual evapotranspiation ratio, F, would be usually higher than 1.0 when the aridity index, ϕ, is larger than 4.0 in the HRC. In the literature, the $F > 1$ cases were also observed when ϕ is just higher than 1.0 (Cheng et al., 2011; Wang, 2012; Chen et al., 2013). Thus, it is interesting to discuss how the occurrence of the $F > 1$ cases is controlled by the catchment properties when shallow groundwater plays an important role.

The equation for the annual evapotranspiation ratio can be derived from Eq. (7) as follows

$$F = (1 - \alpha)\frac{E_1}{P} + \alpha g \frac{E_0}{P} \sum_{m=1}^{12} \left(\frac{E_{0\,m}}{E_0} G_m \right), \tag{21}$$

where E_1 is the annual evapotranspiation in the Zone-1 which is determined by the annual water balance in the soil water reservoir, E_0 and P are the annual potential evaporation and precipitation, respectively. The term $E_{0\,m}/E_0$ denotes the proportion of monthly potential evaporation to the annual one with respect to the mth month. It has been known that the relationship between E_1/P and ϕ in the HRC is similar to that predicted by the conventional Budyko formulas, as shown in Fig. 8, where E_1/P is less

than 1.0. For the groundwater dependent term, defining

$$G_a = \sum_{m=1}^{12} \left(\frac{E_{0m}}{E_0} G_m \right), \tag{22}$$

as the weighted average of the monthly groundwater storage, Eq. (21) can be replaced by

$$F(\phi) = \frac{(1-\alpha)w\phi}{1+w\phi+\phi^{-1}} + \alpha g\phi G_a, \tag{23}$$

where E_1/P is represented by Eq. (5). According to Eq. (23), the function $F(\phi)$ is controlled by the parameters, g, w, α and the status of groundwater represented by G_a. As indicated in Eq. (16), gG_a is a dimensionless parameter to describe the intensity of groundwater dependent evapotranspiration related to the potential evaporation. The recommended range of gG_a is 0.5–1.0.

Typical $F-\phi$ curves obtained with Eq. (23) are given in Fig. 9. It can be seen that the proportion of shallow water table area (α) has large effect on the occurrence of the $F > 1$ case. When the shallow water table area is small ($\alpha = 0.1$), the $F > 1$ case occurs only during extreme dry years. When groundwater dependent evapotranspiration (gG_a) increases, the case $F > 1$ occurs with smaller aridity index. The plant available water coefficient (w) also influences the occurrence of the $F > 1$ case. A larger value of w shifts the $F-\phi$ curves (Fig. 9b) to the left side indicating that the $F > 1$ case could occur with smaller aridity index.

4.3 Using the modified Budyko space

For mean annual water balance, the evapotranspiration ratio is less than 1.0, meaning on long-term average, mean annual evaporation is smaller than mean annual precipitation. However, for the inter-annual and intra-annual water balance, the evapotranspiration ratio is larger than 1.0 during the extreme dry years since groundwater storage

contributes to excess evapotranspiration. Wang (2012) and Chen et al. (2013) argued that it is reasonable to replace the evapotranspiration ratio and the dryness index by $E/(P - \Delta S)$ and $E_0/(P - \Delta S)$, respectively, where ΔS is the storage increment in a studied period. The plots of the annual or seasonal water balances would follow the normal shape in this modified Budyko space. Thus, in this study we attempt to check the characteristics of the annual water balance data in the HRC using such a modified Budyko space. For the ABCD-GE model, the total change in storage for a year was estimated as

$$\Delta S = \sum_{m=1}^{12} [(1 - \alpha)(S_m + V_m - S_{m-1} - V_{m-1}) + (G_m - G_{m-1})], \tag{24}$$

where m is the number of the months in the year, $m - 1$ denotes the storage at the end of the last year. Results are shown in Fig. 10. It can be seen that in the modified Budyko space annual water balance data fall into the zone below the limitation:$E/(P - \Delta S) < 1$, even below the modified Budyko curve obtained with Eq. (2) using the newly defined evapotranspiration ratio and dryness index. Furthermore, the $E/(P - \Delta S)$ value approaches a stable value around 0.90 with the varying $E_0/(P - \Delta S)$ value. It indicates that at least 10 % of $P - \Delta S$ is contributed to the annual runoff, in terms of $Q/(P - \Delta S)$.

4.4 Limitation remarks

Attention should be paid to the simplifications in the conceptual models when the equations and formulas are applied in complicated catchments. The ABCD model assumes that the storage–evapotranspiration relationship is controlled by the parameters a and b whereas the physical interpretation of them is difficult (Alley, 1984). Equation (11) in the ABCD model is also hypothesized from a simplified storage-loss process that controlled by the parameter b (Thomas, 1981). Sankarasubramanian and Vogel (2002) suggested that the b value for annual water balance could be approximately represented by the maximum soil moisture field capacity plus maximum E_0 for $\phi < 1$ or

maximum P for $\phi \geq 1$. The a value is generally estimated in a small range between 0.95 and 1.0. In this study, the model output is not sensitive to the a value. The correlation between a and b may exist because both of them are positively related with $E_m + S_m$ in Eq. (10). The ABCD model neglects the possibility of groundwater-dependent evapotranpiration which has been incorporated in the ABCD-GE model. The ABCD-GDE model clearly divides the area into shallow and deep groundwater zones, without considering a complicated spatial distribution of groundwater depth. For the shallow groundwater zone the evapotranspiration is assumed to be proportional to groundwater storage. Nonlinear behavior in groundwater dependent evapotranspiration could be further included if it has been successfully parameterized. Linear groundwater storage–discharge relationship is adopted in both of the ABCD and ABCD-GE models. These simplifications could cause systematic errors in modeling a catchment where the nonlinear behaviors in the hydrological processes are significant. The models ignore the snow cover process. For catchments in cold region one can refer to Martinez and Gupta (2010) who proposed the snow-augmented ABCD model.

5 Conclusions

The Budyko hypothesis assumes that the evapotranspiration ratio (F) is less than 1 and varies with the aridity index (ϕ) along a Budyko curve determined by a catchment specific parameter. This hypothesis is robust for long-term mean annual water balance but is dubious for the inter-annual variations in catchment with varying dryness. The annual water balance plot for a catchment in the Budyko space could be significantly different from that presumed from the Budyko curves, in particular, when the cases of $F > 1$ occur as that have been observed in a number of catchments.

In this study, we highlighted the effects of groundwater dependent evapotranspiration in triggering the abnormal shift of annual water balance in the Budyko space in comparison with traditional Budyko curves. A conceptual monthly hydrological model, the ABCD-GE model, was developed from the widely used ABCD model to incorporate the

groundwater-dependent evapotranspiration in the zone with shallow water table and delayed groundwater recharge in the zone with deep water table. The model was successfully applied in the Hailiutu River Catchment (HRC) in China where 53 years data of runoff and groundwater discharge are available.

5 The results show that the traditional Budyko hypothesis is not valid for the interannual variability of catchment water balance with groundwater dependent evapotranspiration. The shift of the annual water balance in the Budyko space is a combination of the Budyko-type response in the deep groundwater zone and more stable evapotranspiration in the shallow groundwater zone. Groundwater storage supplies excess evapo-

10 transpiration during extreme dry years. The occurrence of the $E/P > 1$ cases depends on the proportion area of the shallow groundwater zone, the intensity of groundwater dependent evapotranspiration and the catchment properties determining the normal Budyko-type trend in the deep groundwater zone. Water utilization for irrigation may enhance this excess evapotranspiration phenomenon.

References

Arora, V. K.: The use of the aridity index to assess climate change effect on annual runoff, J.
20   Hydrol., 265, 164–177, 2002.
Alley, W. M.: On the treatment of evapotranspiration, soil moisture accounting, and aquifer recharge in monthly water balance models, Water Resour. Res., 20, 1137–1149, 1984.
Budyko, M. I.: Evaporation under natural conditions, Isr. Program for Sci. Transl., Jerusalem, 1948.
25 Budyko, M. I.: The heat balance of the earth's surface, US Department of Commerce, Washington DC, USA, 1958.
Budyko, M. I.: Climate and life, Academic, New York, USA, 1974.

Chen, X. and Hu, Q.: Groundwater influences on soil moisture and surface evaporation, J. Hydrol., 297, 285–300, 2004.

Cheng, L., Xu, Z., Wang, D., and Cai, X.: Assessing interannual variability of evapotranspiration at the catchment scale using satellite-based evapotranspiration data sets, Water Resour. Res., 47, W09509, doi:10.1029/2011WR010636, 2011.

Chen, X., Alimohammadi, N., and Wang D.: Modeling interannual variability of seasonal evaporation and storage change based on the extended Budyko framework, Water Resour. Res., 49, 6067–6078, 2013.

Cohen, D., Person, M., Daannen, R., Sharon, L., Dahlstrom, D., Zabielski, V., Winter, T. C., Rosenberry, D. O., Wright, H., Ito, E., Nieber, J., and Gutowski Jr., W. J: Groundwater-supported evapotranspiration within glaciated watersheds under conditions of climate change, J. Hydrol., 320, 484–500, 2006.

Fan, J., Wang, Q., and Hao, M.: Estimation of reference crop evapotranspiration by Chinese pan, Transactions of the CSAE, 22, 14–17, 2006 (in Chinese).

Fernandez, W., Vogel, R. M., and Sankarasubramanian, A.: Regional calibration of a watershed model, Hydrolog. Sci. J., 45, 689–707, 2000.

Fu, B. P.: On the calculation of the evaporation from land surface, Sci. Atmos. Sin., 5, 23–31, 1981 (in Chinese).

Gerrits, A. M. J., Savenije, H. H. G., Veling, E. J. M., and Pfister, L.: Analytical derivation of the Budyko curve based on rainfall characteristics and a simple evaporation model, Water Resour. Res., 45, W04403, doi:10.1029/2008wr007308, 2009.

Greve, P., Gudmundsson, L., Orlowsky, B., and Seneviratne, S. I.: Introducing a probabilistic Budyko framework, Geophys. Res. Lett., 42, 2261–2269, 2015.

Istanbulluoglu, E., Wang, T. Wright, O. M., and Lenters, J. D.: Interpretation of hydrologic trends from a water balance perspective: The role of groundwater storage in the Budyko hypothesis, Water Resour. Res., 48, W00H16, doi:10.1029/2010WR010100, 2012.

Li, W. and Sankarasubramanian, A.: Reducing hydrologic model uncertainty in monthly streamflow predictions using multimodel combination, Water Resour. Res., 48, W12516, doi:10.1029/2011WR011380, 2012.

Lv, J., Wang, X.-S., Zhou, Y., Qian, K., Wan, L., Derek, E., and Tao, Z.: Groundwater-dependent distribution of vegetation in Hailiutu River catchment, a semi-arid region in China, Ecohydrology, 6, 142–149, 2013.

Shift of annual water balance in the Budyko space

X.-S. Wang and Y. Zhou

Title Page

Abstract | Introduction

Conclusions | References

Tables | Figures

◀ | ▶|

◀ | ▶

Back | Close

Full Screen / Esc

Printer-friendly Version

Interactive Discussion

Mathevet, T., Michel, C., Andreassian, V., and Perrin, C.: A bounded version of the Nash–Sutcliffe criterion for better model assessment on large sets of basins, in: Large Sample Basin Experiments for Hydrological Model Parameterization, Results of the Model Parameter Experiment–MOPEX, IAHS Publ. 307, IAHS Press, Wallingford, Oxfordshire, UK, 211–218, 2006.

Martinez, G. F. and Gupta, H. V.: Toward improved identification of hydrological models: A diagnostic evaluation of the "abcd" monthly water balance model for the conterminous United States, Water Resour. Res., 46, W08507, doi:10.1029/2009WR008294, 2010.

Mezentsev, V. S.: More on the calculation of average total evaporation, Meteorol. Gidrol., 5, 24–26, 1955.

Middleton, N. and Thomas, D. S. G. (Eds.): World atlas of desertification, United Nations Environment Programme, Edward Arnold, London, UK, 1992.

Nash, J. E. and Sutcliffe, J. V.: River flow forecasting through conceptual models part I – A discussion of principles, J. Hydrol., 10, 282–290, 1970.

Porporato, A., Daly, E., and Rodriguez-Iturbe, I.: Soil water balance and ecosystem response to climate change, Am. Nat., 164, 625–632, 2004.

Potter, N. J. and Zhang, L.: Interannual variability of catchment water balance in Australia, J. Hydrol., 369, 120–129, 2009.

Renner, M., Seppelt, R., and Bernhofer, C.: Evaluation of water-energy balance frameworks to predict the sensitivity of streamflow to climate change, Hydrol. Earth Syst. Sc., 16, 1419–1433, 2012.

Roderick, M. L. and Farquhar, G. D.: A simple framework for relating variations in runoff to variations in climatic conditions and catchment properties, Water Resour. Res., 47, W00G07, doi:10.1029/2010WR009826, 2011.

Sankarasubramanian, A. and Vogel, R. M.: Annual hydroclimatology of the United States, Water Resour. Res., 38, 1083, doi:10.1029/2001WR000619, 2002.

Shi, C., Niu, K. Chen, T., and Zhou, X.: The study of pan coefficients of evaporation pans, Sci. Geograpica Sinica, 6, 305–313, 1986 (in Chinese).

Sloto, R. A. and Crouse, M. Y.: HYSEP: a computer program for streamflow hydrograph separation and analysis, US Geological Survey Water–Resources Investigations Report 96–4040, 1996.

Thomas, H. A.: Improved methods for national water assessment, Report, Contract WR 15249270, US Water Resour. Council, Washington DC, 1981.

Vandewiele, G. L., Xu, C.-Y., and Ni-Lar-Win: Methodology and comparative study of monthly water balance models in Belgium, China and Burma, J. Hydrol., 134, 315–347, 1992.

Wang, D.: Evaluating interannual water storage changes at watersheds in Illinois based on long-term soil moisture and groundwater level data, Water Resour. Res., 48, W03502, doi:10.1029/2011WR010759, 2012.

Wang, D. and Tang, Y.: A one-parameter Budyko model for waterbalance captures emergent behaviorin darwinian hydrologic models, Geophys. Res. Lett., 41, 4569–4577, doi:10.1002/2014GL060509, 2014.

Wang, T., Istanbulluoglu, E., Lenters, J., and Scott, D.: On the role of groundwater and soil texture in the regional water balance: An investigation of the Nebraska Sand Hills, USA, Water Resour. Res., 45, W10413, doi:10.1029/2009WR007733, 2009.

Yang, D., Shao, W., Yeh, P. J. F., Yang, H., Kanae, S., and Oki, T.: Impact of vegetation coverage on regional water balance in the nonhumid regions of China, Water Resour. Res., 45, W00a14, doi:10.1029/2008wr006948, 2009.

Yang, D., Sun, F., Liu, Z., Cong, Z., and Lei, Z.: Interpreting the complementary relationship in non-humid environments based on the Budyko and Penman hypotheses, Geophys. Res. Lett., 33, L18402, doi:10.1029/2006gl027657, 2006.

Yang, D., Sun, F., Liu, Z., Cong, Z., Ni, G., and Lei, Z.: Analyzing spatial and temporal variability of annual water-energy balance in nonhumid regions of China using the Budyko hypothesis, Water Resour. Res., 43, W04426, doi:10.1029/2006wr005224, 2007.

Yang, H., Yang, D., Lei, Z., and Sun, F.: New analytical derivation of the mean annual water-energy balance equation, Water Resour. Res., 44, W03410, doi:10.1029/2007WR006135, 2008.

Yang, Z., Zhou, Y., Wenninger, J., and Uhlenbrook, S.: The causes of flow regime shifts in the semi-arid Hailiutu River, Northwest China, Hydrol. Earth Syst. Sc., 16, 87–103, 2012.

Yeh, P. J.-F. and Famiglietti, J. S.: Regional Groundwater Evapotranspiration in Illinois, J. Hydrometeorol., 10, 464–478, 2009.

Yin, L., Zhou, Y., Huang, J., Wenninger, J., Zhang, E., Hou, G., and Dong, J.: Interaction between groundwater and trees in an arid site: Potential impacts of climate variation and groundwater abstraction on trees, J. Hydrol., 528, 435–448, 2015.

York, J. P., Person, M., Gutowski, W. J., and Winter, T. C.: Putting aquifers into atmospheric simulation models: An example from the Mill Creek Watershed, Northeastern Kansas, Adv. Water Resour., 25, 221–238, 2002.

Title Page

Abstract | Introduction

Conclusions | References

Tables | Figures

|◄ | ►|

◄ | ►

Back | Close

Full Screen / Esc

Printer-friendly Version

Interactive Discussion

Zhang, L., Dawes, W. R., and Walker, G. R.: Response of mean annual evapotranspiration to vegetation changes at catchment scale, Water Resour. Res., 37, 701–708, doi:10.1029/2000wr900325, 2001.

Zhang, L., Hickel, K., Dawes, W. R., Chiew, F. H. S., Western, A. W., and Briggs, P. R.: A rational function approach for estimating mean annual evapotranspiration, Water Resour. Res., 40, W02502, doi:10.1029/2003WR002710, 2004.

Zhang, L., Potter, N., Hickel, K., Zhang, Y., and Shao, Q.: Water balance modeling over variable time scales based on the Budyko framework - Model development and testing, J. Hydrol., 360, 117–131, doi:10.1016/j.jhydrol.2008.07.021, 2008.

Zhou, Y., Wenninger, J., Yang, Z., Yin, L., Huang, J., Hou, L., Wang, X., Zhang, D., and Uhlenbrook, S.: Groundwater–surface water interactions, vegetation dependencies and implications for water resources management in the semi-arid Hailiutu River catchment, China – a synthesis, Hydrol. Earth Syst. Sc., 17, 2435–2447, 2013.

X.-S. Wang and Y. Zhou

Full Screen / Esc

Printer-friendly Version

Interactive Discussion

Table 1. Mean annual fluxes in the Hailiutu River catchment (HRC) in different periods.

Periods	P (mm)	E_0 (mm)	Q (mm)	Num. of diversions[*]
1957–1966	387.0	1230.2	42.3	0
1967–1987	337.0	1269.6	32.6	4
1988–1997	329.9	1240.2	23.4	9
1998–2010	352.8	1234.0	28.0	10

[*] According to Yang et al. (2012).

Table 2. Best fitting parameters of the "natural" model for the HRC.

Period	a	b	c	d	g	k	α	Error[*]	NSE
		mm		$\times 10^{-2}$	$\times 10^{-2}$ m^{-1}	$\times 10^{-2}$		(%)	
1957–1966	0.97	33	0.92	4.53	1.00	1.68	0.21	13.9	0.51

[*] Mean standard errors of the monthly runoff and groundwater discharge.
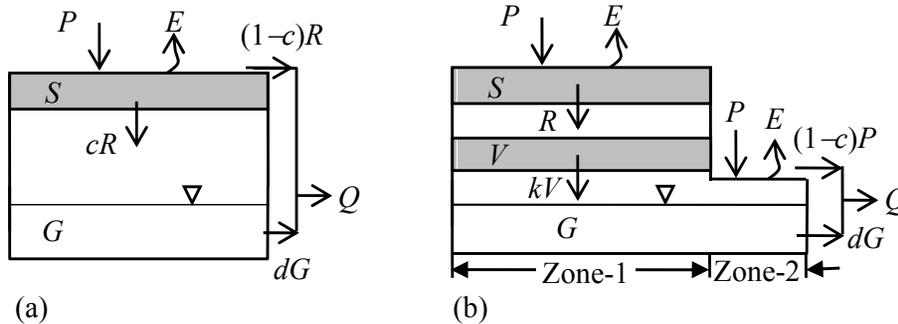
Figure 1. Schematic representations of the ABCD model **(a)** and ABCD-GE model **(b)**. S and V are the effective soil water storage and the effective storage in the transition vadose zone, respectively. G is the effective groundwater storage.
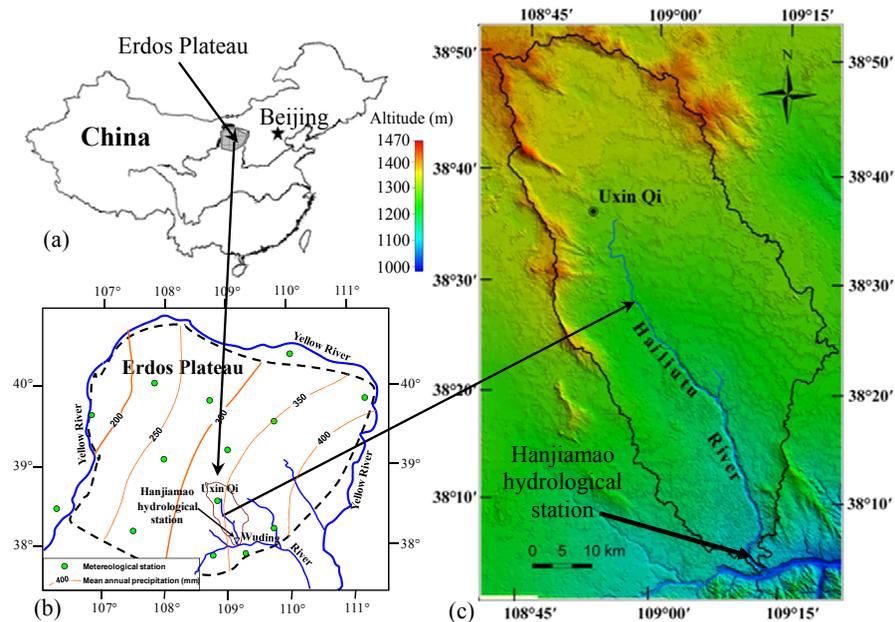
Figure 2. Geographic information of the study site: **(a)** location of the study area in north central China; **(b)** Distribution of meteorological stations in the Erdos Plateau (green points) and contours of mean annual precipitation plotted from 1 km resolution gridded precipitation data; **(c)** Topography of the Hailiutu River catchment represented using a 30 m gridded DEM.

Figure 3. Historgram of requency for groundwater depth in the HRC according to the gridded data of groundwater level in Lv et al. (2013).
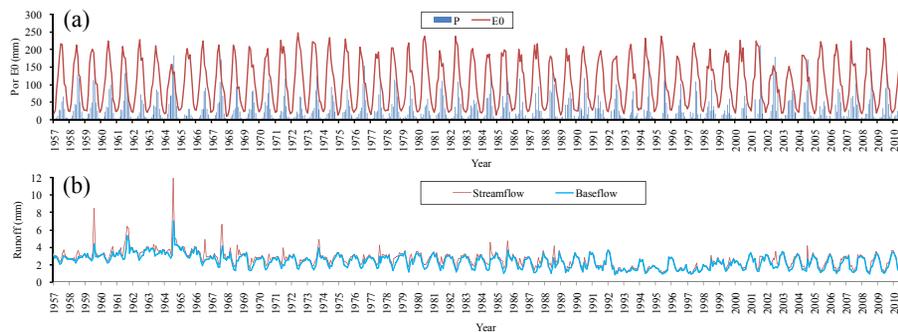
Figure 4. The monthly meteorological data **(a)** and streamflow-baseflow data **(b)** from 1957 to 2010 in the HRC.
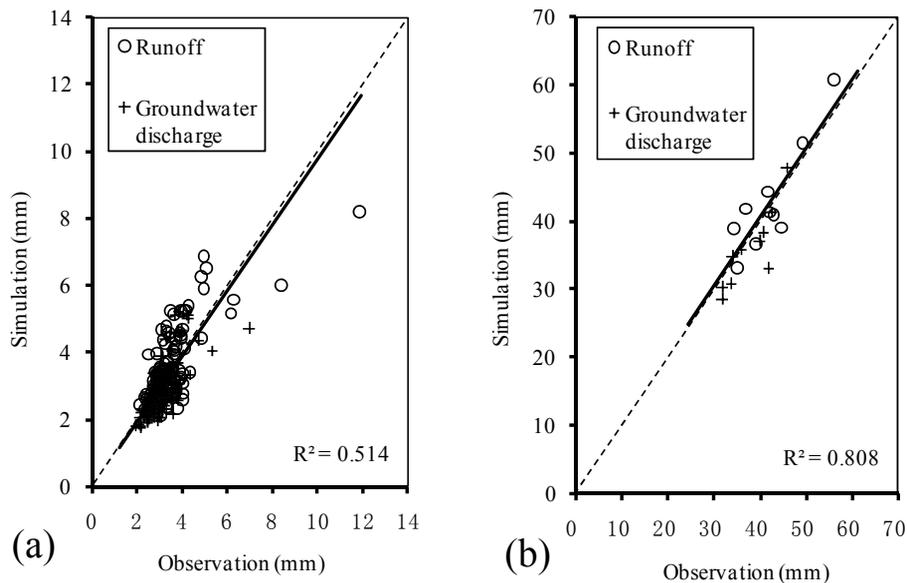
Figure 5. Correlation plots of the observed and simulated monthly **(a)** and annual **(b)** results for the 1957–1966 period.
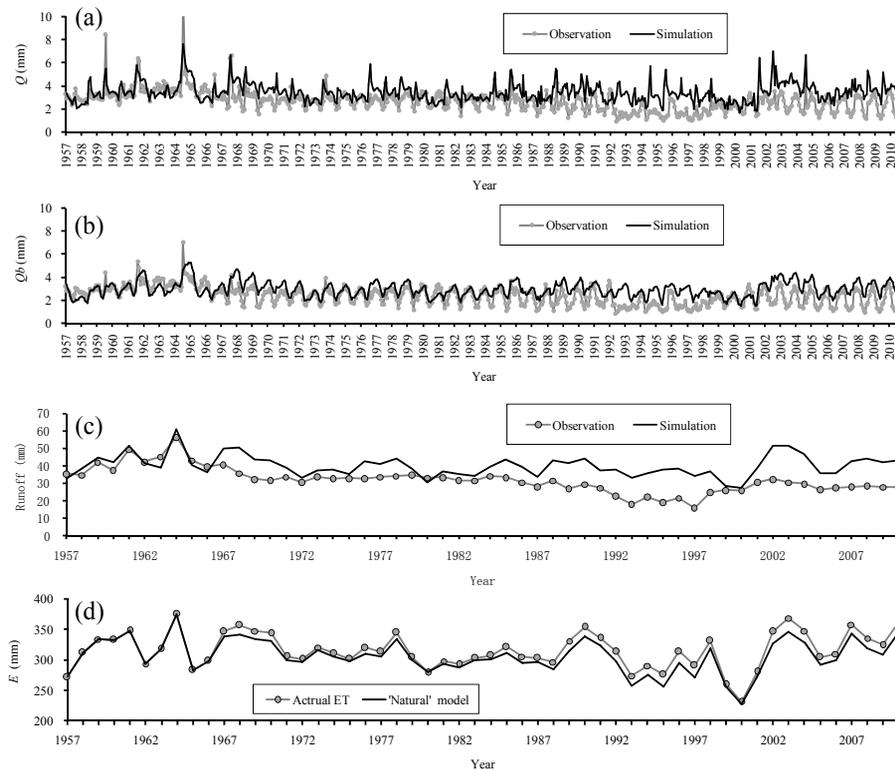
Figure 6. Simulated results of the "natural" ABCD-GE model in comparison with the observation in the HRC from 1957 to 2010, including: Monthly runoff **(a)**, groundwater discharge **(b)**, annual runoff **(c)** and annual evapotranspiration **(d)**. The "natural" model is calibrated with observation data during 1957–1966 when the impacts of human activities are minimum. The actual evapotranspiration in **(d)** was estimated with Eq. (20).

Discussion Paper | Discussion Paper | Discussion Paper | Discussion Paper

Figure 7. Plots of the annual evapotranpiration ratio in the HRC vs. the annual aridity index in the Budyko space **(a)** and the annual runoff ratio vs. the annual aridity index **(b)**. The dashed lines are the linear correlation curves for the "natural" model data.
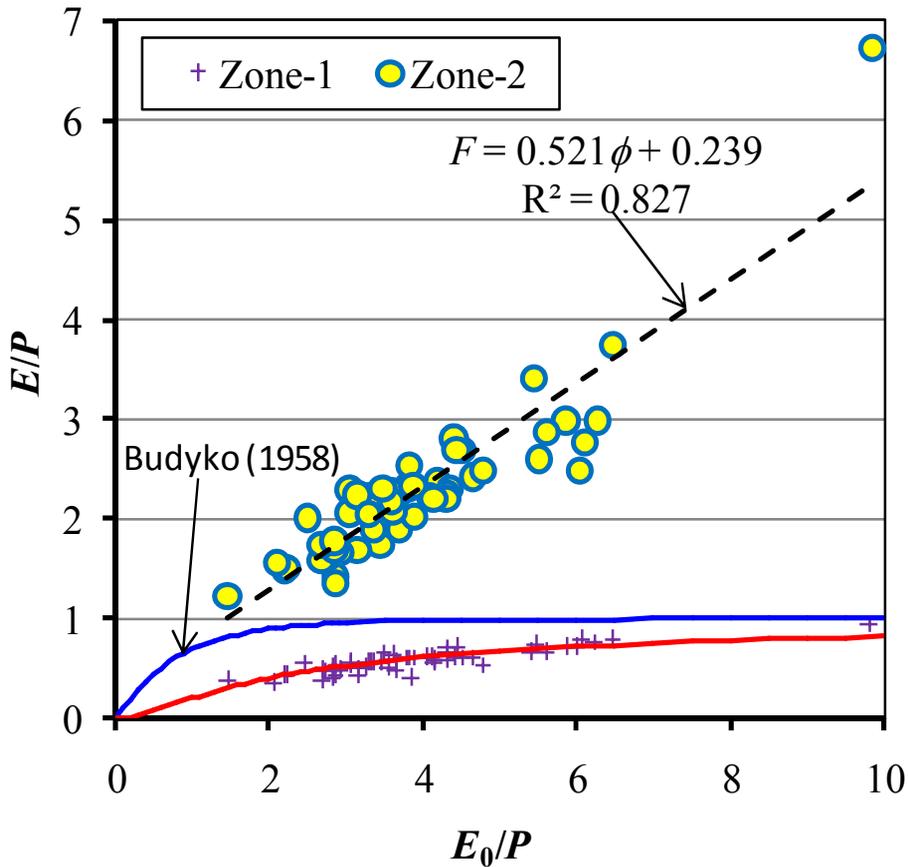
Figure 8. Plots of the annual evapotranpiration ratio in the HRC vs. the annual aridity index in the Budyko space for Zone-1 and Zone-2 based on the "natural" model. The dashed line is the linear correlation curve for the Zone-2 data. The red curve is obtained with Eq. (5) where $w = 0.5$.
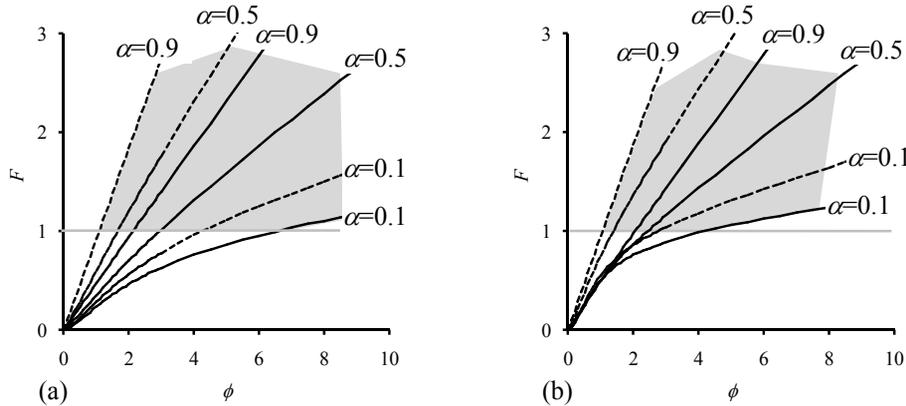
Figure 9. The typical F–ϕ curves for annual water balance in the Budyko space determined with Eq. (23) when $w = 0.5$ **(a)** and $w = 2.0$ **(b)**. The solid and dashed line curves are estimated using $gG_a = 0.5$ and $gG_a = 1.0$, respectively. The gray blocks denote the potential $F > 1$ zones.
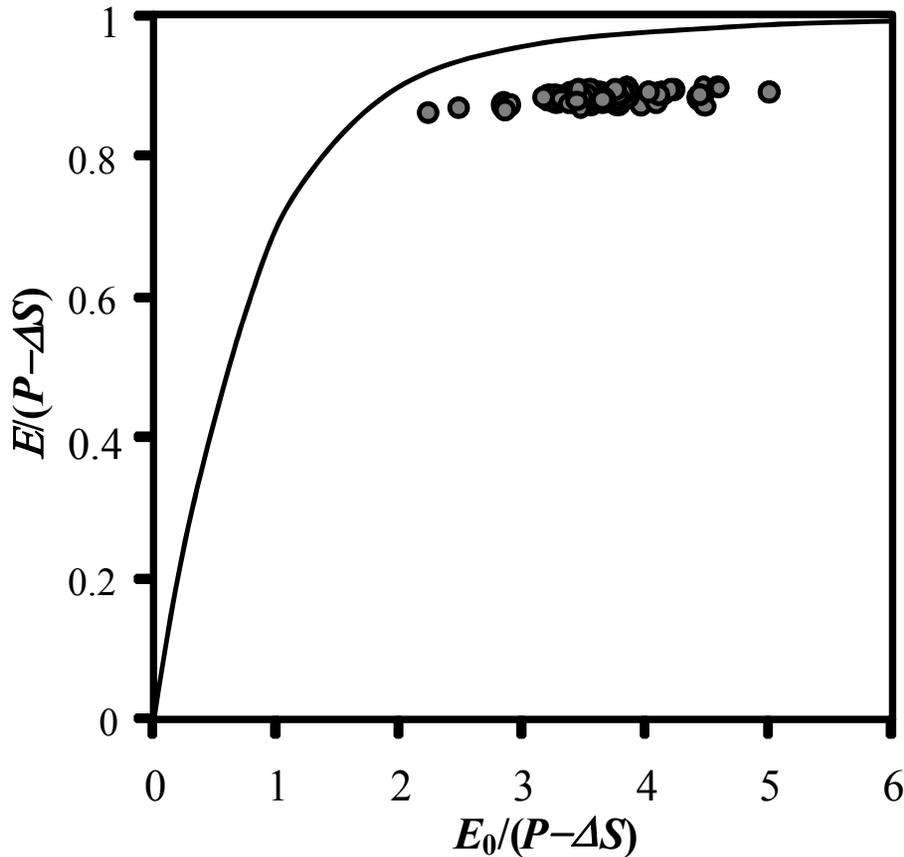
Figure 10. Annual water balance data in the modified Budyko space. Dots are the data obtained for the HRC using the "natural" model. The curve represents the result of Budyko equation (Budyko, 1958) with $E_0/(P - \Delta S)$ and $E/(P - \Delta S)$, respectively, instead of E_0/P and E/P.